International Journal of Thermophysics, Vol. 6, No. 6, 1985

Microscopic Studies of Fluids in Pores: Computer Simulation and Mean-Field Theory[1]

B. K. Peterson,[2] J. P. R. B. Walton,[2,3] and K. E. Gubbins[2]

The behavior of a simple model of a fluid confined to a single, infinitely long cylindrical pore is investigated by means of both a grand canonical Monte Carlo computer simulation and a mean-field theory. The theory is used to calculate the density profile of the fluid, as well as the grand potential of the system. The effect of the (size of the) pore radius as well as the temperature and pressure on the phase behavior of the fluid is studied in some detail, and the results are compared to those produced by related work in this field. The preliminary results from the simulation indicate that, in pores whose radii are a few molecular diameters in size, the fluid molecules tend to pack in cylindrically concentric shells about the axis of the pore.

KEY WORDS: adsorption; capillary condensation; pores; size effects.

1. INTRODUCTION

The study of the behavior of fluids within pores or capillaries is important, from both a practical and a theoretical viewpoint. Practically, it is of interest because many important industrial processes (for example, adsorption [1], separation [2], gas permeability [3], etc.) involve a fluid which is confined to a region that is small on a molecular scale. On the other hand, from a theoretical point of view, it can be expected that the presence of the fluid-wall forces will cause the properties of the fluid in the pore or capillary to be quite different from those of the bulk fluid (in a way that is analogous to the difference between the bulk fluid and, for example,

[1] Paper presented at the Ninth Symposium on Thermophysical Properties, June 24–27, 1985, Boulder, Colorado, U.S.A.

[2] School of Chemical Engineering, Cornell University, Ithaca, New York 14853, U.S.A.

[3] Present address: BP Research Centre, Chertsey Road, Sunbury-on-Thames, Middlesex TW16 7LN, United Kingdom.

0195-928X/85/1100-0585$04.50/0

a fluid between parallel plates [4] or the fluid within a drop or a bubble [5]). In particular, the use of equations derived from classical thermodynamics to predict these properties or to analyze experimental results must be viewed with some suspicion when the system size becomes small, since thermodynamically speaking, the fluid is then no longer well defined [6].

The task of the theoretician in this area, and the problem to which this paper is addressed, is the detailed investigation of these systems using truly microscopically based techniques, with a view to the eventual comparison of these results with those which have a purely thermodynamic origin.

2. METHOD

The theory of fluids (particularly inhomogeneous fluids) has benefited in the past from the comparison of its predictions with the quasi-experimental results obtained from two complementary techniques, namely, computer simulation and the use of simplified model fluids. Before discussing these two techniques, however, let us briefly consider the system which is examined.

We consider a system of spherical molecules, all of the same species, which interact with each other via the potential

$$\begin{aligned} u(r) &= u_{\mathrm{LJ}}(r) - u_{\mathrm{LJ}}(r_c); \qquad r \leqslant r_c \\ &= 0; \qquad r > r_c \end{aligned} \tag{1}$$

where

$$\begin{aligned} u_{\mathrm{LJ}}(r) &= 4\varepsilon[(\sigma/r)^{12} - (\sigma/r)^6] \\ r_c &= 2.5\sigma \end{aligned} \tag{2}$$

the Lennard-Jones function, characterized by a length (σ, the collision diameter) and an energy (ε, the well depth); we use combinations of these to suitably reduce the properties of the system so as to make them dimensionless. The molecules are placed in a cylindrical container of infinite height and radius R and are acted upon by an external potential emitting from the wall of the container. This potential is calculated by (a) assuming that the solid can be modeled as a continuum of density ρ_{SOLID} which is infinite in extent, (b) assuming a Lennard-Jones interaction (with values of σ and ε which are different from those for the fluid–fluid interaction) to exist between each fluid molecule and each volume element in the solid, and (c) integrating this potential over the solid [7]:

$$V(\mathbf{r}) = \int_{\mathrm{SOLID}} d\mathbf{r}'\, u_{\mathrm{LJ}}(|\mathbf{r} - \mathbf{r}'|)\, \rho_{\mathrm{SOLID}} \tag{3}$$

The values of the σ's and the ε's used in the interactions may be chosen to produce reasonable representations of different fluids at different adsorbates; here, we choose to study fluid argon on solid carbon dioxide.

We now discuss the two techniques used. Simulation may be described as a "brute force" route to the properties of interest. They are calculated by using the microscopic equations of statistical mechanics in an assembly of molecules and then averaged over a series of configurations generated by the computer in the appropriate ensemble. In this work, we use the simulation technique known as grand canonical Monte Carlo [8]. Here, the temperature, volume, and chemical potential are chosen, and the simulation calculates the other properties of the system. This type of simulation technique is particularly well suited to the study of phase transitions and adsorption isotherms [9].

In contrast, the development of the model fluid approach starts from the following relationship [10]:

$$\Omega[\rho] = F[\rho] + \int d\mathbf{r}\, V(\mathbf{r})\, \rho(\mathbf{r}) - \mu \int d\mathbf{r}\, \rho(\mathbf{r}) \tag{4}$$

Here, μ is the chemical potential, and $\rho(\mathbf{r})$ is the singlet density at the position $\mathbf{r}$ in the inhomogeneous system. Ω and F are functionals of ρ; Ω has the property that it is minimized by the equilibrium density profile, when it is then the grand potential of the system, and F is then the intrinsic Helmholtz free energy. By minimizing this equation, we obtain, then,

$$\left(\frac{\delta\Omega}{\delta\rho}\right)_{\text{eqm}} = \left(\frac{\delta F}{\delta\rho}\right)_{\text{eqm}} + V(\mathbf{r}) - \mu = 0 \tag{5}$$

This is still only a formal relation, but by constructing a model for F, we can solve it for ρ. The model we choose is [11]

$$F[\rho] = \int d\mathbf{r}_1\, f_{\text{h}}(\rho(\mathbf{r}_1)) + \frac{1}{2} \int d\mathbf{r}_1 \int d\mathbf{r}_2\; u_{\text{a}}(r_{12})\, \rho(\mathbf{r}_1)\, \rho(\mathbf{r}_2) \tag{6}$$

where the first term is a local approximation to the effect of the repulsive forces acting between the molecules; $f_{\text{h}}(\rho)$ is the free-energy density of a hard-sphere fluid of density ρ—here, we use the Percus–Yevick (compressibility) approximation to this quantity. The second term is due to the attractive intermolecular forces which are dealt with using a mean-field approximation; u_{a} is the attractive part of the potential u. We note that this model for F is rather crude in that the short-range order of the fluid is neglected and so, for example, the profiles obtained from this theory for a fluid against a wall will not show the packing effects that are to be found

in, for example, the simulation. More sophisticated models for F overcome this limitation [12]. Using Eq. (6) in Eq. (5) gives

$$\mu_h(\rho(\mathbf{r}_1)) + \int d\mathbf{r}_2\, u_a(r_{12})\, \rho(\mathbf{r}_2) + V(\mathbf{r}_1) - \mu = 0 \tag{7}$$

Given a reasonable starting guess for $\rho(\mathbf{r})$, this equation may be solved for the profile, generally via an iterative procedure. The technical details of the method of solution will be presented elsewhere.

This general expression, Eq. (7), simplifies according to the geometry of the system being studied. Thus, for the pore, $\rho(\mathbf{r}) \to \rho(s)$, a function of (two-dimensional) radius only, and the integral above reduces to a simpler form.

3. RESULTS AND DISCUSSION

The results presented come, for the most part, from the mean-field theory. This is partly because this is faster to implement than the simulation and partly due to the way in which this problem is being tackled, i.e., one of the functions of the theory is to identify areas of interest in the phase diagram and to suggest the most profitable conditions under which to perform simulations.

The applied parameters in both methods are the temperature, the chemical potential, and the volume (or radius) of the pore. It is, however, more convenient to present the results from the theory in terms of the temperature, pressure, and volume, since this affords a more immediate connection with, for example, the adsorption isotherms measured by experimental methods.

Consider the pore at some subcritical temperature and at some pressure at or below that of the saturated bulk fluid. Looking for profiles that satisfy Eq. (7), we find that, for a large pore radius, two different solutions result from the minimization of Ω—one corresponding to a high, liquid-like density at the center of the pore and one corresponding to a low, gas-like density there. Both are local minimina in Ω; to decide which is the absolute minimum, Ω must be calculated explicitly for each, using Eqs. (4) and (6). The one with the lower Ω value is the stable solution, while the other is metastable.

At saturation, we find that, for all temperatures so far studied (down to $kT/\varepsilon = 0.2$), the liquid-filled pore is the stable configuration. Upon decreasing the pressure to below saturation, the vapor configuration becomes more stable than the liquid, provided that the pore radius is large enough. However, as R is decreased, Ω_{vap} remains more or less constant,

but Ω_{liq} falls rapidly. The point at which they cross (see Fig. 1) is the point of transition between the vapor-filled pore and the liquid-filled pore—that is, the point at which capillary condensation occurs. There is a metastable part to the gas branch of the curve, which ends at a radius which is smaller than the transition radius.

Figure 2 shows the density profiles (that is, the stable solutions) at the temperature and pressure of Fig. 1. Increasing the pressure shifts the point of transition to larger radius. Figure 3 shows the adsorption isotherms at $kT/\varepsilon = 0.9$ for a variety of pore radii. Here Γ/L, the adsorption per unit length of pore, is

$$\Gamma/L = 2\pi \int_0^R s\, ds[\rho(s) - \rho_b] \tag{8}$$

where ρ_b is the density of the bulk fluid at the same temperature and pressure. As the pore size increases, the pressure at which the transition from gas to liquid occurs increases, approaching the saturation pressure as $R \to \infty$.

The results which have so far been obtained for the phase equilibria in the pore, according to the mean-field theory, are summarized in Fig. 4. These are the coexistence isotherms, plotted as a function of the pressure and pore radius. We find that altering the temperature has little effect on the radius at which, for a given pressure, the liquid- and the gas-filled pores

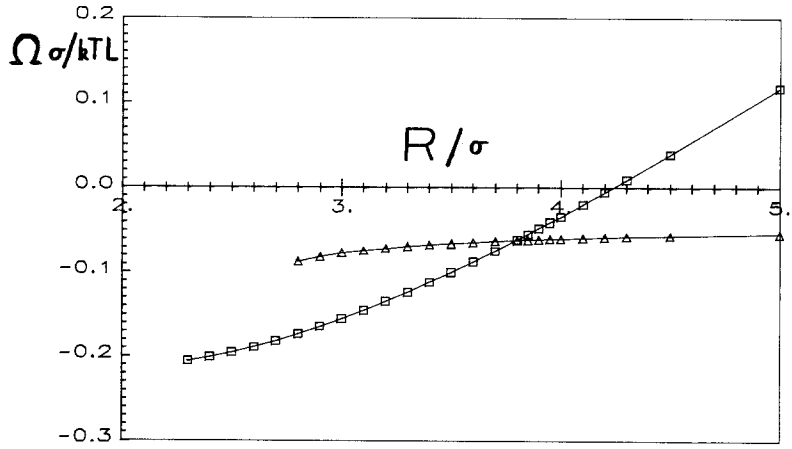

Fig. 1. Reduced grand potential per unit length of pore as a function of reduced pore radius, at $kT/\varepsilon = 0.7$ and $P/P_{\text{sat}} = 0.6$, for the liquid-filled (□) and the vapor-filled (△) pore, calculated from the mean-field theory. The curves cross at the point of transition between the two configurations.

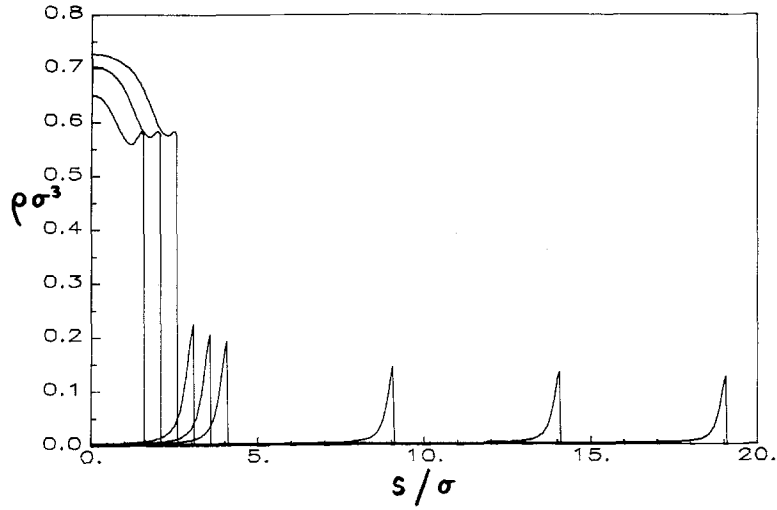

Fig. 2. Reduced density profiles at $kT/\varepsilon = 0.7$ and $P/P_{sat} = 0.6$, from the mean-field theory.

coexist, although it seems as if this radius is weakly proportional to the temperature.

This result may be compared to that of Evans and Tarazona [4], who used this theory to study a fluid whose molecules interact via a (nontruncated) exponential potential placed between two parallel walls which act on

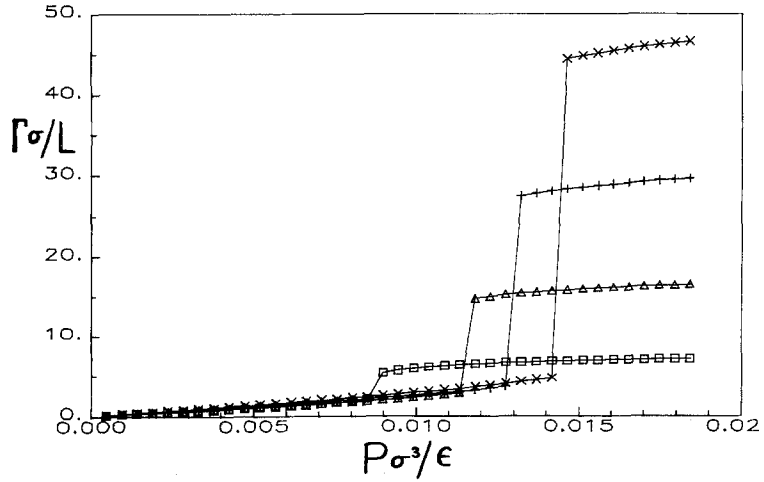

Fig. 3. Plot of reduced adsorption vs reduced pressure at $kT/\varepsilon = 0.9$ and reduced pore radii of 3.0 (□), 4.0 (△), 5.0 (+), and 6.0 (×). Calculated from the mean-field theory.

the fluid via an exponential potential having a range equal to that of the fluid–fluid interaction. They find that this system has a more complicated phase diagram than that shown in Fig. 4, the phase behavior being a strong function of the temperature in their system. The difference between the two sets of results is, perhaps, not too surprising in view of the fact that the behavior of fluids in the neighborhood of a wall has been shown [13] to be extremely sensitive to the fine details of the model used. We note in passing that, by changing the values of the parameters in the potentials to those appropriate to a different fluid at a different adsorbate, it is possible to obtain a phase diagram having a structure that is quite different from that in Fig. 4.

One feature of Evans and Tarazona's results which, however, should apparantly be independent of the details of the potentials is that their coexistence curves terminate on a line of critical points. We have found evidence for the presence of a critical point on the isotherm only at the higher temperatures so far studied ($kT/\varepsilon = 1.0$, 0.9); work is in progress to see if this feature can be observed at the lower temperatures. Similarly, we are currently engaged in a comparison of the predictions of the theory with those of the Kelvin equation (which is purely thermodynamic in its origins), with a view to determining the range of its validity in this system.

Finally, we show in Figs. 5 and 6 two density profiles from the simulation. These results are presented in terms of the temperature, volume, and (excess) chemical potential (over that of an ideal gas at the

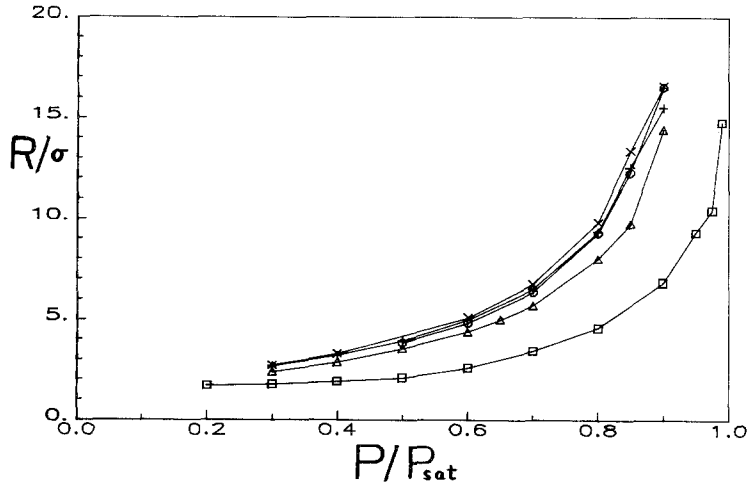

Fig. 4. Coexistence isotherms in the pore, calculated from the mean-field theory, at reduced temperatures of 0.2 (□), 0.3 (△), 0.4 (+), 0.6 (×), and 0.9 (○).

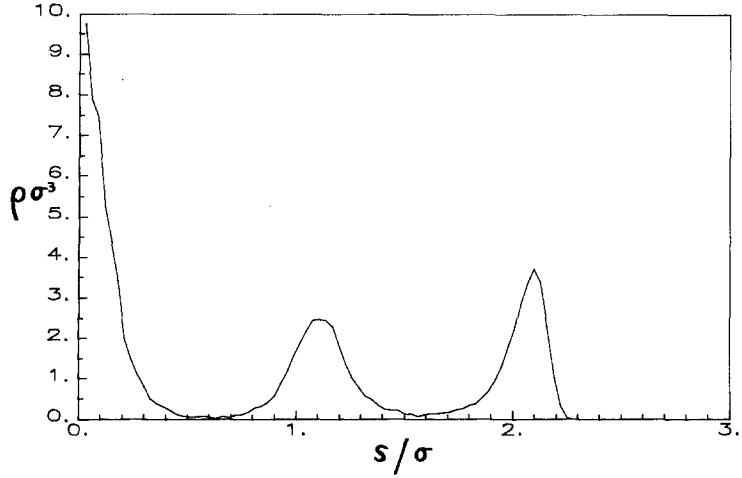

Fig. 5. Reduced density profiles at $kT/\varepsilon = 1.0$, $R/\sigma = 3.0$, and $\mu_{ex}/\varepsilon = -0.1$, from the computer simulation.

same conditions as the bulk phase). Their most striking feature is the pronounced structure, indicating that the molecules are packing in cylindrical shells around the center of the pore (this tendency is, perhaps, aided by the fact that the pores in Figs. 5 and 6 have radii which are an integral number of molecular diameters in size). Although these results are only preliminary, the comparison with the profiles generated by the mean-field theory is perhaps a good demonstration of the point noted above—that a

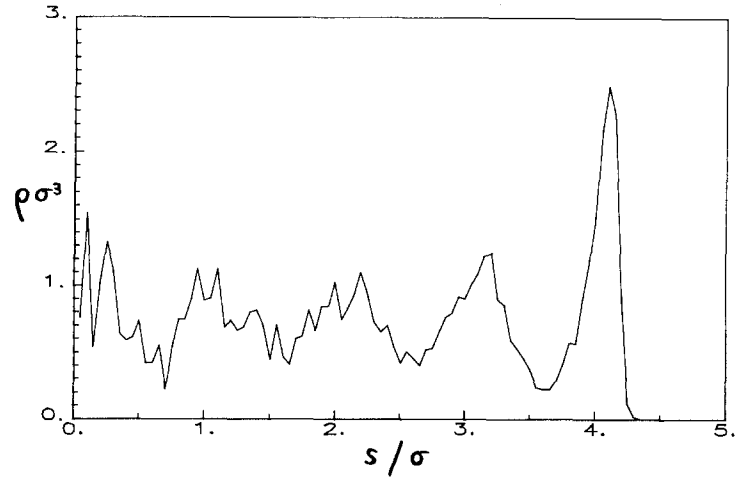

Fig. 6. As for Fig. 5, but with $R/\sigma = 5.0$.

realistic incorporation of the effect of short-range correlations would be a significant improvement in the theory, especially in its description of the behavior of fluids in these pores having radii of only a few molecular diameters. This problem is currently under consideration.

ACKNOWLEDGMENTS

We thank the National Science Foundation (Grant No. CHE-8305056) for financial support of this work and M. M. Telo da Gama for helpful discussions.

REFERENCES

1. D. M. Ruthven, *Principles of Adsorption and Adsorption Processes* (Wiley, New York, 1984).
2. W. J. Schell, *Hydrocarbon Process.*, August issue, p. 43 (1983).
3. J. D. Walls, A. M. Nur, and T. Bourbie, *J. Pet. Tech.*, April issue, p. 930 (1982).
4. R. Evans and P. Tarazona, *Phys. Rev. Lett.* **52**:557 (1984).
5. S. M. Thompson, K. E. Gubbins, J. P. R. B. Walton, R. A. R. Chantry, and J. S. Rowlinson, *J. Chem. Phys.* **81**:530 (1984).
6. J. S. Rowlinson, *Chem. Soc. Rev.* **12**:251 (1983).
7. W. A. Steele and G. D. Halsey, *J. Phys. Chem.* **59**:57 (1955).
8. D. Adams, *Mol. Phys.* **28**:1241 (1974); **29**:307 (1975).
9. D. J. Nicholson and N. G. Parsonage, *Computer Simulation and the Statistical Mechanics of Adsorption* (Academic Press, London, 1982); J. E. Lane and T. H. Spurling, *Aust. J. Chem.* **33**:231 (1980); **34**:1529 (1981); W. van Megen and I. K. Snook, *Mol. Phys.* **54**:741 (1985).
10. J. S. Rowlinson and B. Widom, *Molecular Theory of Capillarity* (Clarendon Press, Oxford, 1982).
11. J. K. Percus, *Trans. N.Y. Acad. Sci.* **6**:1062 (1964); N. G. van Kampen, *Phys. Rev.* **135**:362 (1964); D. E. Sullivan, *Phys. Rev. B* **25**:5532 (1979).
12. P. Tarazona and R. Evans, *Mol. Phys.* **52**:847 (1984).
13. P. Tarazona and R. Evans, *Mol. Phys.* **48**:799 (1983).